Tellus SERIES A DYNAMIC METEOROLOGY AND OCEANOGRAPHY
PUBLISHED BY THE INTERNATIONAL METEOROLOGICAL INSTITUTE IN STOCKHOLM

A comparison of two identification and tracking methods for polar lows

By LAN XIA[1]*, MATTHIAS ZAHN[2], KEVIN I. HODGES[2], FRAUKE FESER[1] and HANS VON STORCH[1], [1]*Institute for Coastal Research, Helmholtz-Zentrum Geesthacht Max-Planck-Str. 1, 21502 Geesthacht, Germany*; [2]*NERC Centre for Earth Observation (NCEO), University of Reading, Reading, UK*

(Manuscript received 29 June 2011; in final form 2 January 2012)

ABSTRACT

In this study, we compare two different cyclone-tracking algorithms to detect North Atlantic polar lows, which are very intense mesoscale cyclones. Both approaches include spatial filtering, detection, tracking and constraints specific to polar lows. The first method uses digital bandpass-filtered mean sea level pressure (MSLP) fields in the spatial range of 200–600 km and is especially designed for polar lows. The second method also uses a bandpass filter but is based on the discrete cosine transforms (DCT) and can be applied to MSLP and vorticity fields. The latter was originally designed for cyclones in general and has been adapted to polar lows for this study. Both algorithms are applied to the same regional climate model output fields from October 1993 to September 1995 produced from dynamical downscaling of the NCEP/NCAR reanalysis data. Comparisons between these two methods show that different filters lead to different numbers and locations of tracks. The DCT is more precise in scale separation than the digital filter and the results of this study suggest that it is more suited for the bandpass filtering of MSLP fields. The detection and tracking parts also influence the numbers of tracks although less critically. After a selection process that applies criteria to identify tracks of potential polar lows, differences between both methods are still visible though the major systems are identified in both.

Keywords: cyclone, tracking algorithm, polar lows, spatial filter, North Atlantic

1. Introduction

Automatic tracking methods provide a convenient way to perform the analysis of weather systems in long-term datasets to explore their spatial and temporal variability (Murray and Simmonds, 1991; Hodges, 1994, 1995; Serreze, 1995; Blender et al., 1997; Gulev et al., 2001; Muskulus and Jacob, 2005; Wernli and Schwierz, 2006; Zahn and von Storch, 2008a). Using numerical-tracking algorithms is essential to objectively detect long-term changes of storms or cyclones. Tracking methods can also enable us to study the formation and the decay of storms or cyclones, as well as a possible merging or separation of cyclones during their lifetime (Inatsu, 2009).

Generally, automatic Lagrangian tracking methods can be divided into three parts: pre-processing (filtering), detection and tracking. In addition, the tracks are classified according to intensity, structure and activity. Spatial filters are often used before storm or cyclone identification to remove the large-scale background (Hoskins and Hodges, 2002; Anderson et al., 2003) and to select the spatial scales of interest, especially for tracking mesoscale and small-scale lows (Zahn and von Storch, 2008a).

The points used for the tracking are typically chosen as local extremes of some field, for example, minima of the mean sea level pressure (MSLP) field (Serreze, 1995; Gulev et al., 2001; Muskulus and Jacob, 2005; Wernli and Schwierz, 2006; Zahn and von Storch, 2008a), the 1000 hPa geopotential height surface (Z1000) (Blender et al., 1997), maxima of the relative vorticity field (Hodges, 1995; Scharenbroich et al., 2010) in the northern hemisphere (NH) and minima in the southern hemisphere (SH) and geostrophic vorticity computed as the Laplacian of pressure or geopotential (Murray and Simmonds, 1991). Typically, the local extrema are detected based on a comparison with the surrounding grid points. The extrema can be found by searching the whole-gridded data using

*Corresponding author.
email: lan.xia@hzg.de

Citation: Tellus A 2012, **64**, 17196, DOI: 10.3402/tellusa.v64i0.17196

a raster scan, but more sophisticated methods can improve the efficiency of the search by first identifying sub-regions. Muskulus and Jacob (2005) segmented pressure fields into areas by a watershed segmentation algorithm and detected minima or maxima in these segmented areas. Wernli and Schwierz (2006) detected minima encircled by at least one closed contour line on Z1000. Scharenbroich et al. (2010) used connected component analysis (CCA) to define locally connected regions with extrema found in every connected region. Similarly, Hodges (1994) used CCA based on hierarchical quad trees.

The next stage links the local extrema to form tracks. Murray and Simmonds (1991) used past motion and pressure tendency to decide the most likely track point at the next time step. Gulev et al. (2001) performed tracking using an interactive approach. Muskulus and Jacob (2005) used a Kalman filtering approach to perform the tracking, which takes into account the whole cyclone history and not just two consecutive time steps to form tracks. Scharenbroich et al. (2010) applied a probabilistic model to decide the most probable tracks of storms. Other simpler methods have also been employed such as those based on nearest neighbour search (Blender et al., 1997). Methods based on the steering-level flow (Marchok, 2002) have also been used. Finally, further criteria are often applied to pick out particular types of cyclones such as some requirements of lifetime or intensity. In this article, selection criteria previously used by Zahn and von Storch (2008a) are applied to both the Hodges and Zahn algorithms to pick out tracks of potential polar lows.

The steps described above will all influence the cyclone track results. The filter range chosen also decides which features will be identified. For a low-pass filter, the long waves will be retained and the track method will select large-scale systems; similarly, a high-pass filter will remove the contributions of long waves and short-wave systems will be tracked. The detection part records the location and values of local extremes, which are used for the tracking. Different techniques and additional requirements in this part can lead to differences in the systems that are identified. The tracking is applied in the next step together with further criteria, which can also affect the final results. For example, Raible et al. (2008) compared three cyclone detection and tracking schemes and found deviations of track length due to different technical aspects in the detection and tracking procedures. Of course, the use of different datasets also influences cyclone characteristics and climatologies. The ECMWF reanalysis (ERA-40) has been shown to produce systematically more cyclones than the NCEP–NCAR reanalysis dataset (Raible et al., 2008) when using MSLP for identification. The study of Feser and von Storch (2008a, b) which used dynamically down-scaled global reanalyses data produced by limited area model showed that lower pressure and higher wind speeds were obtained for typhoon events, which are closer to observations although the tracks of the typhoon events were not improved. The use of different fields and levels has also been shown to result in different numbers of cyclones, even if using the same source dataset (Hoskins and Hodges, 2002). The use of projections for the data can also have an impact on the final results via both identification and tracking. For example, using the standard latitude–longitude projection (plate carrée) preferentially samples the high latitudes (Sinclair, 1997), while distance and direction become distorted relative to their true values on the surface of a sphere. This can be circumvented to some extent by the choice of a different projection and measuring distance and direction on a sphere (Hodges, 1995).

The article examines differences between polar lows identified and tracked by two different methods by comparing the technical features of the filtering, detection and tracking of the two methods. The methods explored are those of Hodges (1994, 1995, 1999) and Zahn and von Storch (2008a). These were applied to detect polar lows in the North Atlantic which are small intense maritime mesoscale cyclones forming poleward of the Polar Front in both hemispheres (Rasmussen and Turner, 2003). Polar lows are associated with intense low-level winds and heavy precipitation and are an important risk factor for maritime operations at high latitudes.

The first tracking method is that of Zahn and von Storch (2008a) which is based on a digital bandpass filter of the MSLP in the spatial range of 200–600 km. The filter was originally designed by Feser and von Storch (2005). This method was especially designed for tracking polar lows. The other method is that of Hodges (1994, 1995, 1999) and uses a bandpass filter based on the DCT and can be applied to MSLP and vorticity fields. The Hodges' programme was designed for tracking weather systems in general but for this study was adapted for tracking polar lows. To make the two algorithms comparable, the settings were adapted to be as similar as possible. The reasons for differences between the two algorithms are studied by comparing distinctive details in filter construction, detection methods and tracking.

In Section 2, we describe the technical details of these two tracking methods and the data we use in this study. Then we show the differences in terms of the filters and detection techniques resulting from applying two methods in Section 3.1, how each part in the tracking process influences the tracks in Section 3.2, and compare tracks of potential polar lows in more detail in Section 3.3. In Section 4, summary and conclusions are given.

2. Description of tracking methods and data

In this section, we compare the two tracking methods in more detail. For abbreviation, we use the acronyms 'MZ' for Zahn and von Storch's (2008a) method and 'KH' for the Hodges' (1994, 1995, 1999) algorithm.

Both methods have three parts: filter, detection and tracking. MZ's algorithm has a fourth part to assign tracks of polar lows according to given constraints and these are also applied to KH's method to identify polar lows.

2.1. Filter

To track polar lows, both tracking methods first apply spatial bandpass filters to extract mesoscale features from the full fields. However, different filter approaches are used. KH uses the DCT based on the discrete Fourier transform with a symmetrisation process (Denis et al., 2002). MZ uses a near-isotropic two-dimensional spatial digital filter (Feser and von Storch, 2005).

Before applying the digital bandpass filter, the trends, determined as quadratic polynomials, were subtracted from the full fields to eliminate possible trends, which could disturb the filtering process (Feser and von Storch, 2005). One difference between the Fourier filter and digital filters is that digital filters are less exact in scale separation than a Fourier filter, as the response function of a digital filter is smooth and not a step function like a Fourier filter (Feser and von Storch, 2005). That means that for bandpass filtering with a digital filter, some contributions of long waves and short waves in the vicinity of the selected wave number boundaries remain. The Fourier filter has some problem when a trend occurs by adding artificial wave contributions; this feature is reduced (but not eliminated) when using the DCT instead.

For the filter used in the MZ method, we use the same configuration as given in Zahn et al. (2008a) to select polar lows more precisely, scales smaller than $\sim$200 km and larger than $\sim$600 km are removed by filtering. Monthly mean fields of MSLP were subtracted before subtracting the quadratic polynomials and applying the digital bandpass filter to reduce the influence of large scales.

KH's filter was originally designed to track synoptic scale cyclones (Hodges, 1994, 1995, 1999), not polar lows. For our comparison studies, we had to reconfigure it in accordance to the dynamics of polar lows. We, therefore, chose the same filter range of 200–600 km to filter MSLP with the DCT.

2.2. Detection

The detection part records all positions of minima or maxima in the filtered output fields below or above given thresholds. Here, MSLP was used for both methods. A threshold value of the bandpass-filtered MSLP smaller than -1 hPa was chosen.

The MZ method was designed to find minima located exactly on the model grid points. The gradient from the cyclone centre has to be larger than 0.3 hPa/100 km. Minima over land are excluded.

The KH method first segments fields into distinct regions by connected component labelling and then it detects extremes in each region (Hodges, 1994, 1995). KH finds minima that are located between grid points by using B-spline interpolation (Dierckx, 1981) and steepest ascent maximization. This results in smoother tracks.

2.3. Tracking

The next step is to link the detected positions to form tracks. In the KH method, the tracks are initialised based on a nearest neighbour method that links the points in consecutive time steps, which in this study are 3 h apart (3 h) if their distance is less than 2° (about 222 km). A cost function is constructed to measure the track smoothness, which is determined over three consecutive time steps and summed along the tracks (Hodges, 1994, 1999). This is minimised subject to constraints on displacement and track smoothness to gain the greatest smoothness, which is performed both forward and backwards in time. The smoothness constraints are applied adaptively so that the constraint is looser if the system moves slowly and stricter if the system moves fast (Hodges, 1999). For MZ, the maximum travel distance for a vortex in a time step is considered to be smaller than 200 km. If more than one position is detected for the next time step, and they all fulfil the maximum distance requirement, the closest one to the current track is chosen. In this study, the tracks have to last at least 1 day (eight time steps) to be retained, this is a post-tracking filter on the lifetimes.

2.4. Polar low criteria

After the application of the aforementioned procedures, there are many tracks that are not all polar lows. In order to identify the polar lows, further criteria are applied as described in Zahn and von Storch (2008a). The criteria that have to be fulfilled are as follows: (1) filtered MSLP should be below -2 hPa at least once along a track (polar lows are strong mesoscale cyclones); (2) the maximum 10 m wind speed within a distance of 100 km around the storm centre has to be larger than 13.9 m s^{-1} at least for 20% of the positions (polar lows are with strong surface wind speeds); (3) the temperature difference between the sea surface temperature and the 500 hPa temperature (T_{500}) must exceed 43 C at least once along the track (in general,

polar lows are thermal instability systems); (4) the detected tracks taking paths along coastal grid boxes for more than 50% of their time are discarded (Zahn et al. (2008) suggested that the filtering procedure can be influenced by mountainous orography along coastlines and there might be some 'artificial' polar lows induced over the orography); (5) a southward moving track, i.e., the first detected position has to be about 100 km farther north than the last (polar lows typically occur with cold air outbreaks and mostly take a southward path but some possible polar lows might be excluded by this criterion) and (6) if the filtered MSLP falls below -6 hPa at least once along the track and criterion (4) is fulfilled, it will also be regarded as a polar low track; otherwise, it should fulfil all five criteria given above. It assumes that a very strong mesoscale disturbance is found and overrides other criteria. These criteria are similar to what are used operationally.

2.5. Data

The data used in this article were produced for a previous study on long-term polar low frequency (Zahn and von Storch, 2008b) by downscaling from the NCEP/NCAR reanalyses (Kalnay et al., 1996). The downscaling was performed by means of a regional climate model called CLM (since renamed to COSMO-CLM, www.clm-community.eu) version 2.4.6 and using spectral nudging as well as providing the boundary conditions from the reanalysis. The CCLM is the climate version of the 'Lokal Modell' of the German Weather service (Steppeler et al., 2003; Rockel et al., 2008). The model uses a longitude–latitude grid of 184 and 72 points, respectively, on a rotated grid with 0.44° and an integration time step of 240 s. The MSLP output used in this study is saved every 3 h. The simulation period is from 1 January 1948 to February 2006 and the simulation area covers Greenland and the Barents Sea in the East, the ice edge prone to shallow baroclinicity in the north and extends to about the position of the Polar Front in the south (Zahn and von Storch, 2008b). In this study, we used two years' data (October 1993 to September 1995) to compare the two methods' abilities to identify and track polar lows.

3. Results

3.1. Filter and detection

In this part, we compare the two filtering and detection parts of the respective methods. The MSLP field is used as an example to show the differences between the digital filter and the DCT.

As a case study, we consider the polar low called Le Cygne (the swan), which developed early on 14 October 1993 mainly because of baroclinic instability over the Barents Sea, then moved equator ward along the Norwegian coast and disappeared after landing in Southern Norway on 16 October 1993 (Grønås and Kvamstø, 1995; Zahn et al., 2008). Figure 1 shows the MSLP field at its genesis stage as a trough at around 72 N, 5–10 E at 06 UTC 14 October. From the satellite images at 1529 UTC 14 October (Fig. 2), this polar low initially displays a distinct comma cloud signature and the developing disturbance is like a swan figure in the cloud fields over the Norwegian Sea (Claud et al., 2004), hence the name.

Figure 3a shows the filtered MSLP field at 06 UTC, filtered with the digital filter of Feser and von Storch (2005), which is used by MZ, on 14 October 1993. Fig. 3b is the filtered MSLP field at the same time but filtered with the DCT from KH. The mesoscale disturbances become more distinct after bandpass filtering. The initial stage of Le Cygne, which is not easy to see in the unfiltered data, becomes more obvious in the filtered fields (marked with a circle in Fig. 3a and b).

There are large differences between both filtered fields. For the digital-filtered field, there is a margin around the model domain with values of 0, as the digital filter needs data in a symmetric neighbourhood around a point to be filtered (Feser and von Storch, 2005). For comparison reasons, this margin zone was cut off for the DCT-filtered fields (Fig. 3b). The digital-filtered MSLP field shows distinct mesoscale systems but still has a similar pattern to the unfiltered MSLP field (Fig. 1). Even subtracting the monthly mean fields of MSLP before filtering does not completely remove the large-scale background. The reason for this is that the response function of the digital filter is smooth with no exact cut-off at the band boundaries and will retain some long-wave parts in the vicinity of the selected band boundaries as described in Section 2.1. We also applied the digital filter and the DCT to the 850 hPa vorticity (Fig. 4) and the filtered patterns are much more similar for both filters than for MSLP, this is because the large-scale background for vorticity is much weaker than it is for MSLP. The MSLP is more influenced by large-scale systems, and even a small portion of large scales retained will affect the filter results greatly. So, the DCT is more effective in an exact scale selection than the digital filter and it is more suitable for MSLP.

The differences between the two fields produced by the two different filtering methods may lead to differences in the numbers and detected locations of the minima. The green points in figures 3a and b are the detected minima using the MZ method and the red squares are the detected minima using the KH method. Most of the green points almost coincide with red squares for both filtered fields but with some minima over land only found by the KH method. This is because, as mentioned before in Section

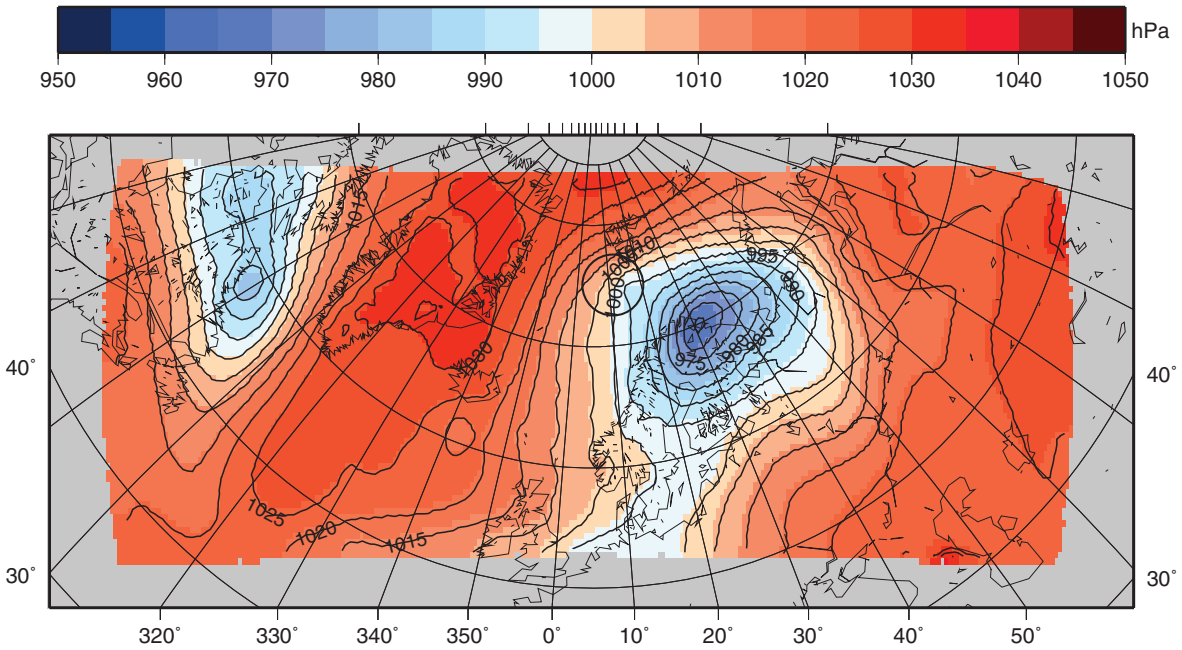

Fig. 1. Unfiltered MSLP field on 06:00 14 October 1993 (hPa).

2.2, the MZ method just detects minima over sea and excludes the minima over land. The fact that there is such a good correspondence between the points detected by both methods results from the data being at such a high resolution. It should be also noted that the MZ detection part uses a gradient criterion to exclude systems with a weak pressure gradient. This compares the surrounding grid points and keeps those minima, which fulfil the gradient criterion. This could lead to fewer minima. To make the two methods comparable in this study, the gradient criterion is set to 0.0 hPa/100 km in the MZ detection part.

3.2. *Comparison of both methods*

In this part, we show how different parts of the whole tracking set-up influence the tracking results by comparing both methods. Table 1 shows the number of tracks obtained for different combinations of filter, detection and tracking parts of the MZ and KH methods. The polar low criteria described in Section 2.4 are not applied at this stage. All the numbers shown in Table 1 are based on the MSLP from October 1993 to September 1995. Several combinations of filter, detection and tracking parts were tested with changing settings for these individual parts according to both MZ and KH methods.

Different settings in the detection can lead to large differences in track numbers between KH and MZ. To make both methods comparable, a gradient of 0.0 hPa/100 km was chosen in MZ and tracks over land were dismissed in KH. Analszing the track numbers in Table 1 for different combinations of filtering, detection and tracking shows that they can be very different. It should be noted, however, that if the filter and tracking parts are the same, the track numbers are more similar between using KH detection and MZ detection. The greatest difference is 115 between combinations 1 and 6 and the smallest difference is 21 between combinations 4 and 7. If the filter and detection parts are the same, the track numbers are also similar between using the KH and the MZ tracking: the greatest difference is 152 between combinations 5 and 6 and the smallest difference is 23 between combinations 1 and 2. In contrast with the detection and tracking parts, the filter leads to larger differences in track numbers. The digital filter used in MZ leads to more tracks than the DCT in KH: the largest difference is 653 between combinations 1 and 3 while the smallest is 567 between combinations 2 and 4. This shows that the detection and tracking parts do not lead to large differences between MZ and KH but the filter does. However, not all these tracks are necessarily polar lows.

In order to identify common tracks between the different combinations, a simple track-to-track comparison algorithm was applied. It defines common tracks as two tracks (with points, which correspond to the same times), which overlap for greater than 60% of their points with mean separation distance of less than 3° and a closest distance less than 100 km at least once. Fig. 5 shows the common tracks of the MZ method applied to data derived from the different filters for October 1993: red lines are tracks of MZ

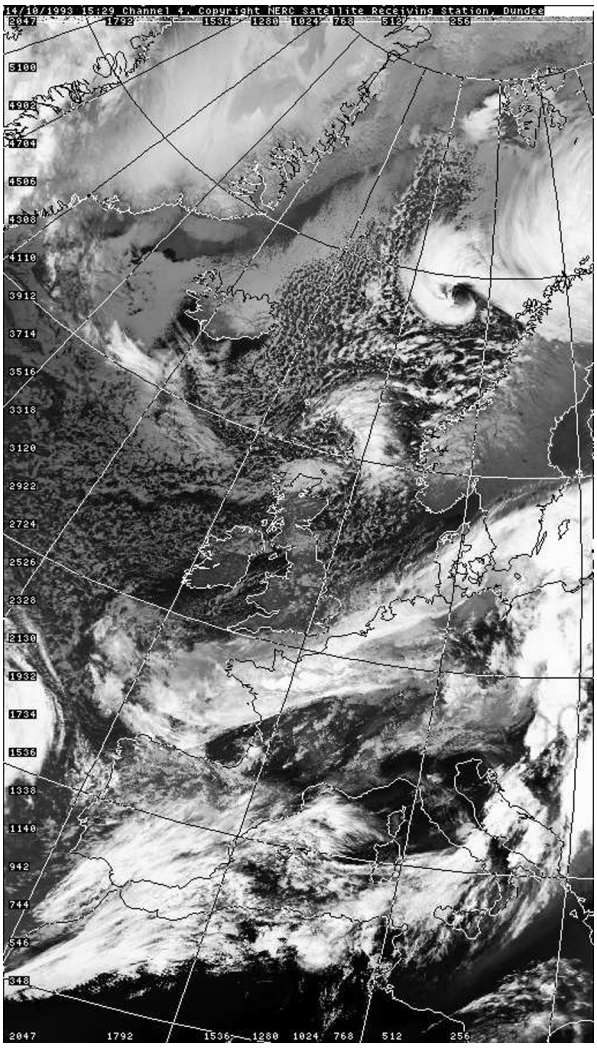

Fig. 2. NOAA 11/AVHRR channel 4 thermal infrared for 1529 UTC 14 October 1993 (from www.sat.dundee.ac.uk/).

using the digital filter (combination 7) and the blue ones are for MZ with the DCT filter (combination 5).

A quantitative measure of the matched and non-matched tracks is provided by the probability of track overlap. The probability P_o of the overlap between two sets of tracks is defined as $P_o = 2N_o/(N_1 + N_2)$, where N_1 and N_2 are the numbers of tracks in the two different combinations, N_o is the number of common tracks between the two track sets. $P_o = 0$ indicates the two sets of tracks are completely different and $P_o = 1$ indicates that the same tracks are present in both sets. The second probability that can be determined is P_m, the probability of non-overlapping tracks and is defined as: $P_m = (N_1 + N_2 - 2N_o)/(N_1 + N_2)$, where $P_m > 0$ means that there is no perfect match between the two track sets. Table 2 shows the probability of common tracks based on comparing different combinations with combination 1, the complete KH method, as the reference. Table 3 is the same with combination 7, the complete MZ method, as the reference.

The highest P_o with combination 1 is combination 2, over 90% of the tracks are common. The only difference between combinations 1 and 2 is the tracking part. The highest P_o with combination 7 is combination 8, over 83% of the tracks are common. The only difference is the tracking part. The tracking parts of both methods lead to comparable numbers and to a lot of common tracks. The second highest P_o with combination 1 is combination 6 and with combination 7 is combination 4. The difference in the methods here is in the detection part. The detection part of MZ with a gradient setting of 0.0 hPa/100 km is similar to that of KH and leads to a small difference in numbers and also to many common tracks. This confirms the analysis given above, that the detection and tracking parts are not the main reasons for differences.

It is notable that in Table 2 the combinations based on the DCT filter such as combination 1 have slightly higher probabilities P_o (over 70%), such as combinations 2, 5 and 6, while combinations with the digital filter (combinations 3, 4, 7 and 8) find only about 30% tracks to overlap with combination 1. Similar results are found in Table 3. Combinations based on the digital filter such as combination 7 also have relatively higher probabilities P_o.

3.3. *Tracks of potential polar lows*

After connecting the minima to form tracks, the numbers of tracks are still too high and not all are polar lows. To identify the polar lows, further criteria are required to select the tracks of potential polar lows. Therefore, in this section, we apply further criteria as given in Zahn and von Storch (2008a), which are also described in Section 2.4. These are applied in an additive way to tracks, which result from applying the MZ and KH methods. Table 4 shows the selection results based on combinations 1, 3, 5 and 7 of Table 1.

After applying the polar low identification criteria, the numbers of tracks identified by the KH and MZ methods differ mostly because of the use of different filters. The KH method based on the DCT gives 84 potential polar lows and based on the digital filter gives 135 potential polar lows; the MZ method based on the DCT filter gives 79 and 127 potential polar lows based on the digital filter. More tracks are retained based on the digital filter than based on the DCT filter. But for the same filter, the numbers of tracks are much closer even for different detection and tracking methods. Differing mesoscale systems are retained by the DCT filter and the digital filter. So variables, such as filtered wind speed, temperature or MSLP, which are used to describe various mesoscale systems, also differ. These

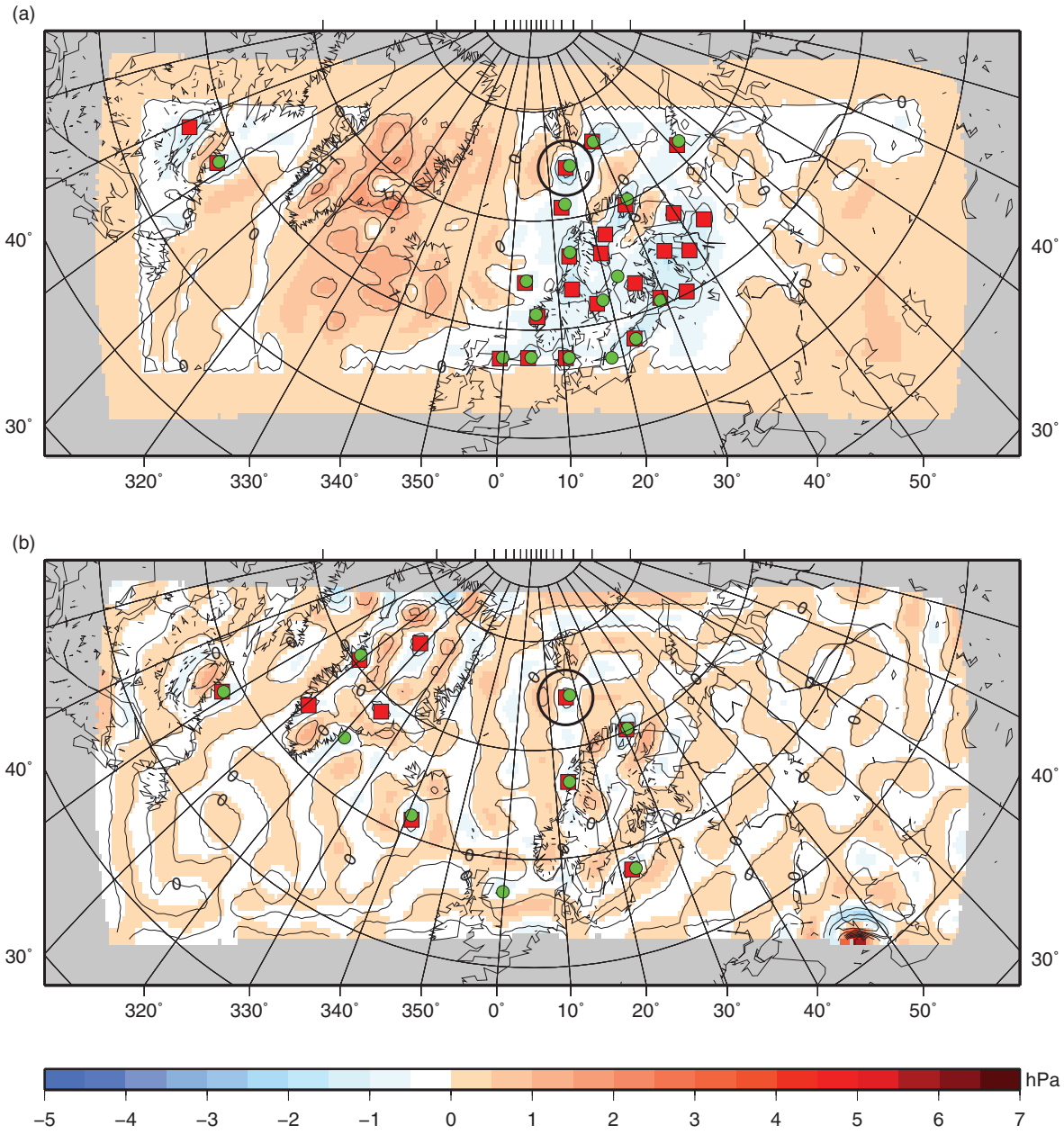

Fig. 3. Bandpass filtered MSLP fields on 06:00 14 October 1993 (hPa): (a) digital filter, (b) DCT, and detected minima: red by KH and green by MZ.

differences lead to the varying track numbers after applying further criteria.

The incremental implementation of the polar low identification criteria has the following impact on the number of systems. The 'filtered minimum' constraint dismisses 38 and 46% of all tracks from combinations 1 and 3 (Table 4), which use the detection and tracking of KH but DCT and digital filters and returns 533 and 818 tracks, respectively. For the MZ detection and tracking applied to the DCT and digital filters, this constraint dismisses 46 and 48% of tracks, as shown in Table 4 for combinations 5 and 7. The vertical stability (vst) criterion dismisses 55 and 53% of the tracks for the KH detection and tracking using the DCT and the digital filter, respectively. For the MZ method, it dismisses 56% of tracks using the DCT and 55% using the digital filter. This criterion is a stronger criterion than the previous two and can dismiss over half of the tracks resulting from both methods. The strongest constraint is the directional criterion, which requires the tracks to go from north to south (by

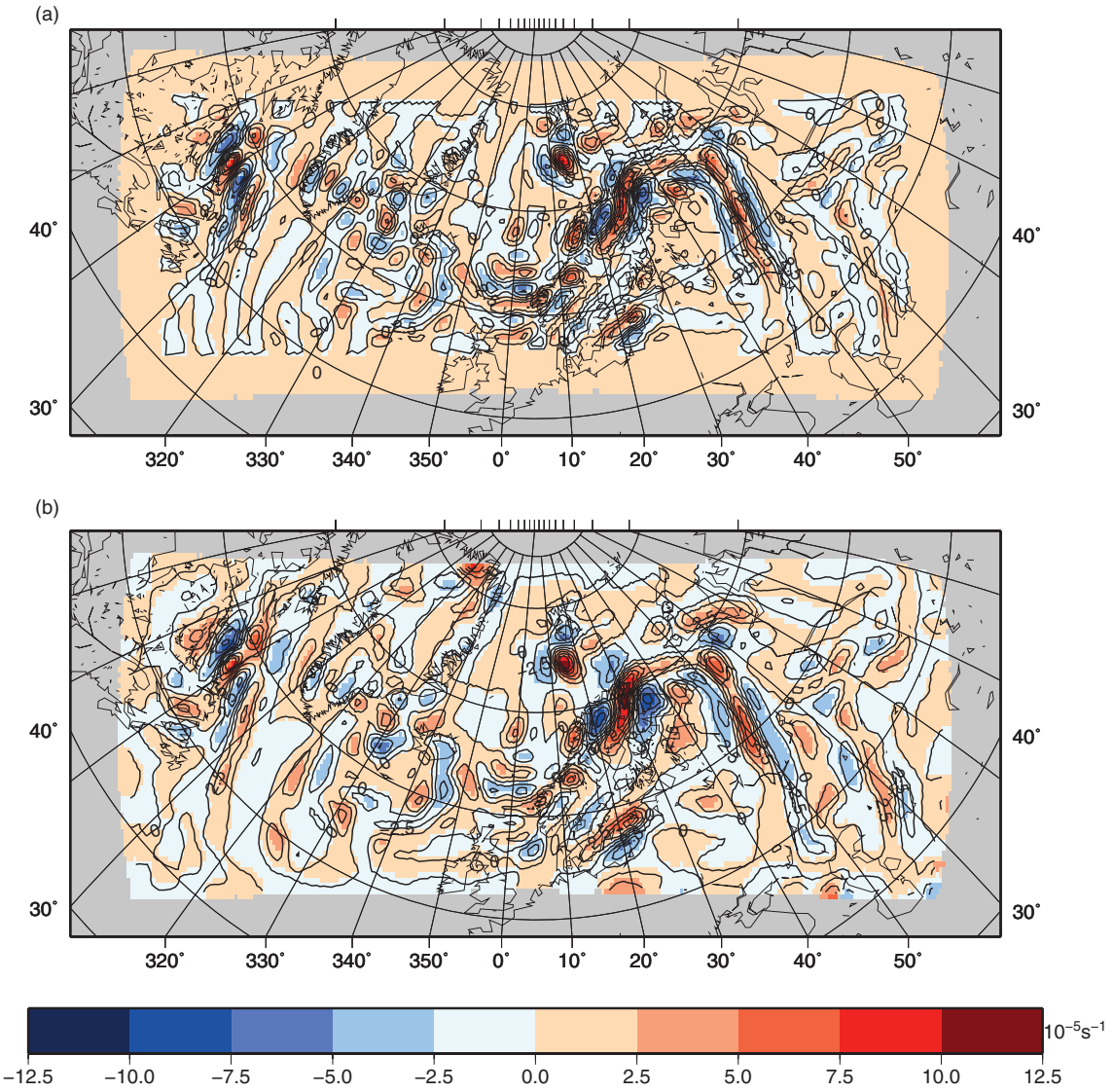

Fig. 4. Bandpass filtered 850 hPa relative vorticity fields on 06:00 14 October 1993 ($10^{-5}\,s^{-1}$): (a) digital filter and (b) DCT.

the acronym 'NS'). It dismisses 65, 64, 58 and 60% of the tracks, respectively, for combinations 1, 3, 5 and 7 in Table 4. The 'wind speed' criterion reduces the numbers by 5, 9, 5 and 8% of the tracks for each combination in Table 4.

Table 1. Numbers of tracks resulting from different combinations between MZ and KH (October 1993 to September 1995)

	Filter	Detection	Tracking	Numbers of tracks
1	KH	KH	KH	856
2	KH	KH	MZ	833
3	MZ	KH	KH	1509
4	MZ	KH	MZ	1400
5	KH	MZ	MZ	819
6	KH	MZ	KH	971
7	MZ	MZ	MZ	1421
8	MZ	MZ	KH	1570

The last criterion of 'supmin' means that the filtered MSLP minima falls below −6 hPa at least once along the track and that the 'noland' criterion is fulfilled. Even if the other criteria are not fulfilled and this criterion is fulfilled, the track is considered a polar low. Table 4 shows that for the DCT filter and the KH detection and tracking, there are three tracks fulfilling the 'supmin' criterion and there is one track for the MZ detection and tracking, which fulfil this criterion. Using the digital filter, there are eight tracks for the KH method and seven tracks for the MZ method that fulfil this criterion. This criterion highly depends on the filter method. The DCT retains less deep low-pressure systems than the digital filter.

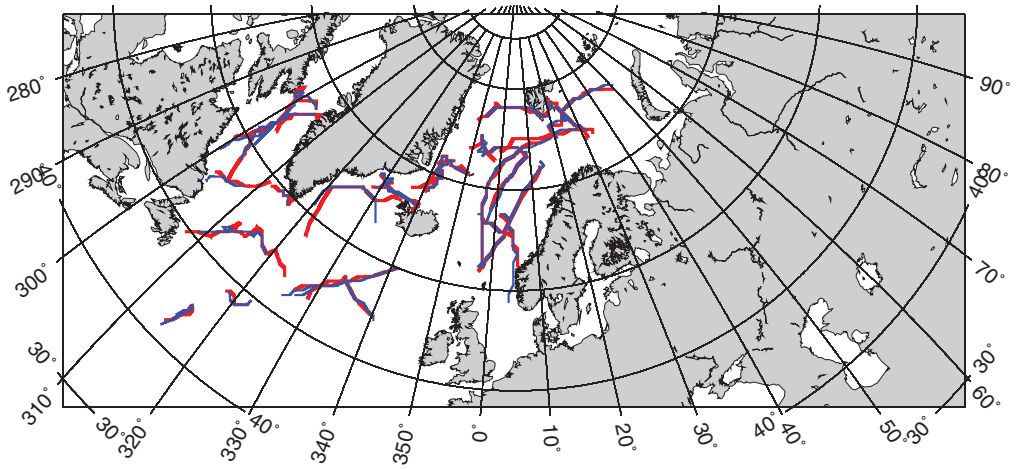

Fig. 5. Overlapping tracks in October 1993 for combination 5 (blue) and combination 7 (red) of Table 1.

Table 2. Number N_o of overlapping tracks, probability P_o for overlapping tracks and ratio P_m of non-overlapping tracks for different combinations in Table 1 using combination 1 as a reference

	1	2	3	4	5	6	7	8
N_o	856	768	385	387	608	713	372	380
P_o	1.00	0.91	0.33	0.34	0.73	0.78	0.33	0.31
P_m	0.00	0.09	0.67	0.66	0.27	0.22	0.67	0.69

Table 3. Number N_o of overlapping tracks, probability P_o for overlapping tracks and ratio P_m of non-overlapping tracks for different combinations in Table 1 using combination 7 as a reference

	1	2	3	4	5	6	7	8
N_o	372	377	989	1025	401	416	1421	1247
P_o	0.33	0.33	0.68	0.73	0.36	0.35	1.00	0.83
P_m	0.67	0.67	0.32	0.27	0.64	0.65	0.00	0.17

Table 4. Numbers of retained potential polar lows after applying the respective criteria in Section 2.4 in October 1993 to September 1995

	Noland	Filtered minimum	Wind speed	vst	NS	supmin	sum
1	856	533	508	231	81	3	84
3	1509	818	744	352	127	8	135
5	819	442	419	186	78	1	79
7	1421	738	680	303	120	7	127

'Noland' means that it excludes tracks over the land as applying the criterion 4; 'filtered minimum' means that filtered MSLP should be below –2 hPa at least once along a track as applying the criterion 1; 'wind speed' means that the maximum 10 m wind speed around the storm centre has to be larger than 13.9 m s^{-1} at least for 20% of the positions as applying the criterion 2; 'vst' means that vertical instability should be fulfilled as applying the criterion 3; 'NS' requires the tracks to go from north to south as applying the criterion 5 and 'supmin' means that the filtered MSLP falls below −6 hPa at least once along the track and 'noland' is also fulfilled as applying the criterion 6. 'Sum' is the final number of retained potential polar lows

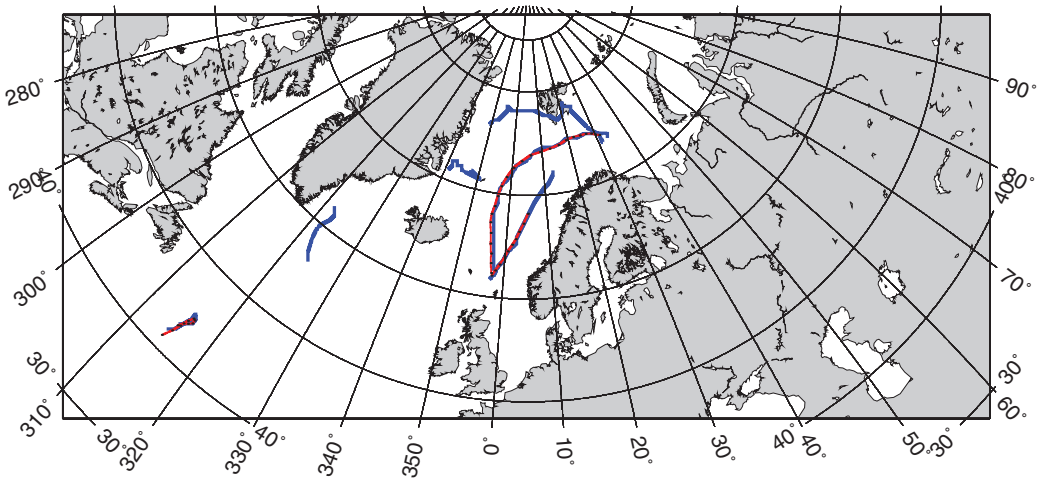

Fig. 6. Tracks of potential polar lows after applying criteria to combination 1 (red with points) of KH and combination 7 of MZ in October 1993 (blue).

For other combinations shown in Table 1, using the same filter leads to comparable numbers, e.g., combination 2 returns 79 tracks of potential polar lows, which is the same as combination 5 whilst combination 4 gives 124 tracks, which is close to the numbers of combination 7.

Figure 6 shows one month's (October 1993) tracks of potential polar lows after applying the polar low identification criteria to combination 1 (red) of KH and combination 7 (blue) of MZ. Combination 1 gives three tracks, while combination 7 leads to six tracks. Three tracks are almost overlapping for both methods. One track of combination 7, which parallels the Norwegian coast over the Norwegian Sea overlaps partly with a track of combination 1 in the Southern Norwegian Sea. The other two tracks generally overlap very well for both combinations. The track of Le Cygne which appeared south of Spitsbergen and decayed at the Southern Norwegian coast is tracked well by both methods.

It is notable that applying the criteria to pick out tracks of potential polar lows still retains the differences of numbers based on the DCT and digital filters. The 'vst' and 'NS' criteria are the most powerful constraints for both methods and can dismiss more than half of the remaining tracks.

4. Conclusions

In this article, two methods for tracking polar lows are compared. Using different filters leads to varying track numbers. If the gradient criterion of MZ detection part is set to 0, the detection part and tracking part between both methods show only small differences in track numbers for the same spatial filter. The polar low identification criteria of MZ were applied to both techniques to assign tracks to potential polar lows. After applying these criteria, the differences in track numbers and locations are still very dependent on spatial filter selection.

The digital filter used by MZ is less precise at scale separation according to wave numbers. These contain large values that influence the filter result even if only small-wave remnants are left over after digital filtering. So, we suggest that the DCT filter is more suited especially for MSLP fields. The filtered vorticity fields obtained by the digital and DCT filters are much more similar, hence it might be expected that smaller differences might occur between detected polar lows obtained by the KH and MZ methodssss when applied to this field. Future work will explore this issue to see if the spatially filtered vorticity is a better alternative to the spatially filtered MSLP by applying both the KH and MZ methods to the vorticity.

5. Acknowledgements

The climate version of the 'Lokal Modell' is the community model of the German climate research (COSMO-CLM, www.clm-community.eu). The NCEP/NCAR reanalysis data were provided by the National Centre for Atmospheric Research (NCAR). This work is a contribution to the Helmholtz Climate Initiative REKLIM (Regional Climate Change), a joint research project of the Helmholtz Association of German research centres (HGF). This work was funded by the China Scholarship Council (CSC) and Institute for Coastal Research Helmholtz-Zentrum Geesthacht within the framework of the Junior Scientist Exchange Program organised by the CSC and

the HGF. The authors thank two anonymous reviewers for constructive comments that helped to improve this article.

References

Anderson, D., Hodges, K. I. and Hoskins, B. J. 2003. Sensitivity of feature based analysis methods of storm tracks to the form of background field removal. *Mon. Weather Rev.* **131**, 565–573.

Blender, R., Fraedrich, K. and Lunkeit, F. 1997. Identification of cyclone-track regimes in the North Atlantic. *Quart. J. Roy. Meteor. Soc.* **123**, 727–741.

Claud, C., Heinemann, G., Raustein, E. and Mcmurdie, L. 2004. Polar low le Cygne: satellite observations and numerical simulations. *Quart. J. Roy. Meteor. Soc.* **130**, 1075–1102.

Denis, B., Cote, J. and Laprise, R. 2002. Spectral decomposition of two-dimensional atmospheric fields on limited-area domains using the discrete cosine transform (DCT). *Mon. Weather Rev.* **130**, 1812–1829.

Dierckx, P. 1981. An algorithm for surface-fitting with spline functions. *IMA J. Numer. Anal.* **1**(3), 267–283.

Feser, F. and von Storch, H. 2005. A spatial two-dimensional discrete filter for limited-area-model evaluation purposes. *Mon. Weather Rev.* **133**, 1774–1786.

Feser, F. and von Storch, H. 2008a. A dynamical downscaling case study for typhoons in SE Asia using a regional climate model. *Mon. Weather Rev.* **136**(5), 1806–1815.

Feser, F. and von Storch, H. 2008b. Regional modelling of the western Pacific typhoon season 2004. *Meteorol. Z.* **17**(4), 519–528.

Grønås, S. and Kvamstø, N. 1995. Numerical simulations of the synoptic conditions and development of arctic outbreak polar lows. *Tellus* **47A**, 797–814.

Gulev, S. K., Zolina, O. and Grigoriev, S. 2001. Extratropical cyclone variability in the Northern Hemisphere winter from the NCEP/NCAR reanalysis data. *Clim. Dyn.* **17**, 795–809.

Hodges, K. I. 1994. A general method for tracking analysis and its application to meteorological data. *Mon. Weather Rev.* **122**, 2573–2586.

Hodges, K. I. 1995. Feature tracking on the unit sphere. *Mon. Weather Rev.* **123**, 3458–3465.

Hodges, K. I. 1999. Adaptive constraints for feature tracking. *Mon. Weather Rev.* **127**, 1362–1373.

Hoskins, B. J. and Hodges, K. I. 2002. New perspectives on Northern Hemisphere storm tracks. *J. Atmos. Sci.* **59**, 1041–1061.

Inatsu, M. 2009. The neighbor enclosed area tracking algorithm for extratropical wintertime cyclones. *Atmos. Sci. Lett.* **10**, 267–272.

Kalnay, E., Kanamitsu, M., Kistler, R., Collins, W., Deaven, D. and co-authors. 1996. The NCEP/NCAR 40-year reanalysis project. *Bull. Am. Meteorol. Soc.* **77**, 437–471.

Marchok, T. P. 2002. How the NCEP tropical cyclone tracker works. Preprints, *25th Conference on Hurricanes and Tropical Meteorology*, San Diego, CA, *Am. Meteor. Soc.*, 21–22.

Murray, R. J. and Simmonds, I. 1991. A numerical scheme for tracking cyclone centres from digital data Part I: development and operation of the scheme. *Aust. Meteor. Mag.* **39**, 155–166.

Muskulus, M. and Jacob, D. 2005. Tracking cyclones in regional model data: the future of Mediterranean storms. *Adv. Geosci.* **2**, 13–19.

Raible, C. C., Della-Marta, P. M., Schwierz, C. and Blender, R. 2008. Northern Hemisphere extratropical cyclones: a comparison of detection and tracking methods and different reanalyses. *Mon. Weather Rev.* **136**, 880–897.

Rasmussen, E. and Turner, J. 2003. *Polar Lows: Mesoscale Weather Systems in the Polar Regions*. Cambridge University Press, Cambridge.

Rockel, B., Will, A. and Hense, A. 2008. The regional climate model COSMO-CLM (CCLM). *Meteorol. Z.* **17**(4), 347–348.

Scharenbroich, L., Magnusdottir, G., Smyth, P., Stern, H. and Wang, C. 2010. A Bayesian framework for storm tracking using a hidden-state representation. *Mon. Weather Rev.* **138**, 2132–2148.

Serreze, M. C. 1995. Climatological aspects of cyclone development and decay in the arctic. *Atmos. Ocean* **33**(1), 1–23.

Sinclair, M. R. 1997. Objective identification of cyclones and their circulation intensity, and climatology. *Weather Forecast.* **12**, 591–608.

Steppeler, J., Doms, G., Schättler, U., Bitzer, H., Gassmann, A. and co-authors. 2003. Meso-gamma scale forecasts using the nonhydrostatic model LM. *Meteorol. Atmos. Phys.* **82**, 75–96.

Wernli, H. and Schwierz, C. 2006. Surface cyclones in the ERA-40 dataset (1958–2001). Part I: novel identification method and global climatology. *J. Atmos. Sci.* **63**, 2486–2507.

Zahn, M. and von Storch, H. 2008a. Tracking polar lows in CLM. *Meteorol. Z.* **17**(4), 445–453.

Zahn, M. and von Storch, H. 2008b. A long-term climatology of North Atlantic polar lows. *Geophys. Res. Lett.* **35**, L22702.

Zahn, M., von Storch, H. and Bakan, S. 2008. Climate mode simulation of North Atlantic polar lows in a limited area model. *Tellus* **60A**, 620–631.